**Zeitschrift:** IABSE reports = Rapports AIPC = IVBH Berichte
**Band:** 63 (1991)

**Artikel:** Current acoustic velocity profiler for coastal monitoring
**Autor:** Whitehouse, Ian / Imberger, Jörg
**DOI:** https://doi.org/10.5169/seals-48508

# Current Acoustic Velocity Profiler for Coastal Monitoring
## Surveillance de la côte au moyen d'un procédé acoustique
## Küstenüberwachung mittels einer akustischen Methode

**Ian WHITEHOUSE**
Proj. Mgr
Univ. of Western Australia
Nedlands, Australia

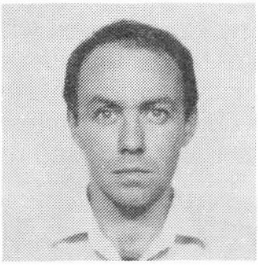

Ian Whitehouse, born 1959, received a B.E at the Univ. of Western Australia in 1983. Since then he has worked in both the United Kingdom and Australia on a variety of projects utilising digital signal processing in the speech/ secondary radar/acoustics fields. His current position at the Centre for Water Research as a principal investigator involves him in a variety of environmental monitoring projects.

**Jörg IMBERGER**
Prof. of Environm. Eng.
Univ. of Western Australia
Nedlands, Australia

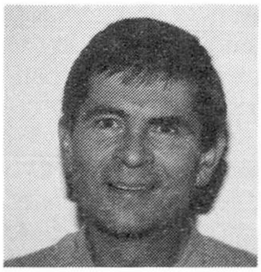

Jörg Imberger, born 1942, received his PhD at the Univ. of California, Berkely, and returned to Australia where he has been a Prof. in the Dep. of Civil and Environmental Engineering at the Univ. of Western Australia since 1978. He is the Director of the Centre for Water Research, and the main theme of his research is the study of mixing in a stratified fluid, specifically concerning the quality of water in estuaries, reservoirs and lakes.

**SUMMARY**

A coherent backscatter velocity profiling sonar is described which uses pseudo random tone modulation and pulse pair processing to extend the range velocity ambiguity product. The consequences of pseudo random tone modulation and detection on the range resolution and the coherence time of the backscattered signal is presented with practical results obtained from laboratory tests. The functional implementation of the instrument and its novel signal generation technique is described with emphasis placed on the system reconfigurability under software control. Practical results obtained with the instrument in field trials are presented. The role of the instrument in coastal monitoring and the management of water resources and future multi-dimensional implementations of the instrument outlined.

Surveillance de la côte au moyen d'un procédé acoustique

Résumé

L'article présente une technique et un instrument de surveillance de la côte basée sur un principe acoustique. Des détails techniques sont donnés. Le rôle de cet instrument, ses applications futures possibles et la gestion des ressources en eau dans les zones côtière sont présentés.

Küstenüberwachung mittels einer akustischen Methode

Zusammenfassung

Der Artikel präsentiert eine Technik und ein Instrumentarium der Küstenüberwachung, das auf einem akustischen Prinzip basiert. Technische Einzelheiten werden gegeben. Seine zukünftigen möglichen Anwendungen für die Rolle dieses Instrumentariums und die Verwaltung der Gewässerresourcen in den Küstenzonen werden dargestellt.

## ABSTRACT

A coherent backscatter velocity profiling sonar is described which uses pseudo random tone modulation and pulse pair processing to extend the range velocity ambiguity product. The consequences of pseudo random tone modulation and detection on the range resolution and the coherence time of the backscattered signal is presented with practical results obtained from laboratory tests. The functional implementation of the instrument and its novel signal generation technique is described with emphasis placed on the system reconfigurability under software control. Practical results obtained with the instrument in field trials are presented. The role of the instrument in coastal monitoring and the management of water resources and future multi-dimensional implementations of the instrument outlined.

## INTRODUCTION

The Acoustic Doppler Current Meter (ADCM) is a backscatter coherent Doppler sonar used to derive water velocities as a function of depth in rivers and coastal waters. The instrument also incorporates a conventional echo ranging function allowing the instrument to monitor water depth or bottom profile as a function of time. The instrument was developed in response to specific requirements :

(i) provide a low cost, accurate method of estimating water velocity as a function of depth
(ii) provide a reliable method of estimating the bed/water/surface interface so as to monitor depth/scour in rivers and around structures.

The development commenced in February 1989 as a two stage, two year project. Stage one would deal with the preliminary research and lead to the construction of a laboratory prototype while stage two would then build on that work and develop a field prototype. Stage one was successful in demonstrating the principles involves and stage two is now nearly complete with the instrument currently undergoing field trials.

The instruments requirements can be summarised as

(i) able to resolve velocities up to a velocity range ambiguity limit of 25 $m^2\ s^{-1}$
(ii) a velocity resolution of 5 mm $s^{-1}$
(iii) a spatial resolution of 20 mm
(iv) able to simultaneously detect the surface/water/bed interface with a spatial resolution of 10 mm

Figure 1 shows a typical deployment application of the ADCM.

## BACKGROUND

The interrelationships of the different types of sonars and the ADCM is shown in Fig. 2. Backscatter Doppler sonars all operate on the principle of echoes from suspended particles and density discontinuities in the acoustic path being reflected back to the source. The principle is shown diagrammatically in Fig. 3 where echoes from a transmitted pulse (starting at t = 0) are reflected from an ensonified bin and then received at time $t_e$ (travel time to and from the ensonification). The Doppler shift, caused by the motion of particles in the bin is then derived by observing the phase shifts between adjacent echoes relative to the phase coherent interrogating pulses. The velocity of the particles in the bin and hence the accompanying water can then be derived.

Coherent Doppler sonar are subject to performance limitations caused principally by (i) a finite propagation speed for acoustic energy and (ii) Nyquists criteria for sampled waveforms. Together they form what are known as the range-velocity ambiguity equations [7] for $r_m$, the maximum resolvable range, and $v_m$, the maximum resolvable velocity.

$$f_d = \frac{2.v_r.f_c}{c}$$ the Doppler shift, $f_d$, from a radial velocity $v_r$, given a carrier frequency $f_c$ and the speed of sound, c. (1)

$$r_m = \frac{c}{2.PRF}$$ a pulse cannot be transmitted before the previous echo has arrived limiting the maximum resolvable range with the pulse repetition frequency, PRF. (2)

$$v_m = \frac{c.PRF}{4.f_c}$$ the resulting Doppler frequency must not exceed a phase shift greater than $\pi$ radians between adjacent interrogating pulses (Nyquists criteria) otherwise a velocity ambiquity will result. (3)

or combining (2) and (3)

$$v_m \, r_m = \frac{c^2}{8 \, f_c} \tag{4}$$

Additionally when considering the performance of coherent Doppler sonars the range resolution must be considered. The range resolution or bin size, $r_e$, is shown in Fig. 3 and defined [1] as

$$r_e = c.t_w$$ where $t_w$ is the temporal width of the transmitted pulse. (5)

Upon consideration of the above equations it can be seen that the above objectives are particularly stringent in relation to the instrument requirements. The acoustic beam can be directed at an angle of 45 ° relative to the bed giving a $1/\sqrt{2}$ reduction in the maximum unambiguous velocity, however, the unambiguous range velocity product is still

$$v_m . r_m = \frac{5.5}{\sqrt{2}} = 17.67$$

which, upon substituting into (4) gives a carrier frequency of 15.9 kHz. Such a low carrier frequency is impractical because of (i) the resulting low spatial resolution and (ii) the required transducer diameter for an adequately small beamwidth. The spatial resolution would be determined by the period of 15.9 kHz in a (say) ten cycle burst of 15.9 kHz i.e. 610uS corresponding to a spatial resolution of 943 mm. Similarly the beamwidth for a piston transducer is given by

$$BW = \frac{91440}{(fc.d)}$$ where BW is the beamwidth in degress and d is the transducer diameter (6)

implying a diameter of 575 mm for a 10° beamwidth (ignoring the near/far field of such a large transducer). The low carrier frequency is obviously impractical.

A more attractive carrier frequency in terms of the beamwidth, spatial resolution, propagation loss and transducer availability would be 300 kHz. A 30 mm transducer would then have a beamwidth of 10° and a ten cycle burst at 300 kHz would exhibit a spatial resolution of 50 mm. Unfortunately, the range velocity product would then be only 0.9375. A factor of 19 below the specified.

Therefore, although coherent backscatter sonars initially seem applicable, it is not possible to simultaneously retain a sufficiently high range velocity ambiguity product, narrow beamwidth, and high spatial resolution to meet the design parameters. Modifications to the basic system were necessary to ensure a practical instrument.

## ACOUSTIC DOPPLER CURRENT METER

To enhance the applicability of the coherent Doppler sonar, two methods of extending $v_m$ and $r_m$ are utilised in the ADCM.

(i) Independent pulses
The range ambiguity restriction is based on the premise of a single pulse traversing the acoustic path between the transducer and the target volume at any one time. This is valid if consecutive pulses are identical because echoes from following transmitted pulses would interfere with echoes from the specified volume. If, however, the pulses were coded and the received "matched" to a specified pulse it would be possible to discriminate between echoes. The ADCM uses transmitted pulses composed of independent m-sequences phase modulating the carrier [3]. M-sequences have a number of desirable properties for the ADCM including ease of implementation, however, other possible coding schemes do exist, Barker [10], Golay [4] and complementary [8].

M-sequence possess (i) good cross correlation properties between sequences [9] and (ii) optimal autocorrelation properties. The first property determines the degree of relation between successive pulses and therefore the signal to noise ratio at the matched received whilst the second has the effect of redefining the range resolution. The autocorrelation of a non-circular m-sequence [2] can be shown to be maximal at zero shift i.e. R(0) with maximal sidelobes of $1/\sqrt{N}$ where N is the length of the sequence. The range resolution and range ambiguity for a sonar using m-sequences as the transmitted pulses can be redefined as

$$r_e = c \,.\, t_c \qquad \text{where } t_c \text{ is the chip length} \tag{7}$$

and $t_w = n \,.\, t_c$ i.e. n is the number of chips in the sequence

$$r_m = \frac{m.c}{2.PRF} \qquad \text{where m is the pulse multiplicity i.e. the number of pulses traversing the path simultaneously} \tag{8}$$

(ii) Frequency pair processing
The velocity ambiguity restriction is based on a finite pulse repetition frequency when interrogating a volume. If a velocity greater than the ambiguity limit is encountered then the resultant measured velocity $v_{measured}$ will "wrap around" or be aliased modulo $v_m$. The number of times a velocity has wrapped over the $v_m$ limit is termed the aliasing order. The apparent velocity is then

$$v_{measured} = v_{actual} \text{ modulo } v_m$$

or

$$v_{actual} = k \,.\, v_m + v_{measured} \tag{9}$$

where k is the aliasing order.

The $v_m$ limit is determined by both the carrier and pulse repetition frequency. It is possible, with certain constraints, to combine two uniquely aliased estimates to unwrap or dealias the measured velocity to its true magnitude. The aliased estimates may be obtained by interrogating the same volume and varying either the pulse repetition or carrier frequency. Varying or staggering the PRF is frequently used [6], however, we chose to vary the carrier frequency. Varying the carrier frequency [1] has implementation advantages in terms of system complexity, however, it also allows the PRF to be retained as a maximum (see later consequences of independent pulses) over the two successive interrogations. If the two interrogations occur with consecutive high and low carrier frequency we have

$$v_{ml} = \frac{c.PRF}{4\, f_{cl}} \qquad v_{mh} = \frac{c.PRF}{4\, f_{ch}} \tag{10}$$

where $v_{ml}$, $v_{mh}$ are the maximum unambiguous velocities for the two carrier frequencies $f_{cl}$ and $f_{ch}$

$$v_{actual} = k_1 \, v_{ml} + v_{measuredlow}$$

$$v_{actual} = k_2 \, v_{mh} + v_{measuredhigh}$$

If we now introduce the constraint that

$$\frac{f_{cl}}{f_{ch}} = \frac{j}{j+1} \tag{11}$$

for j any positive non-zero integer then

$$v_{md} = \frac{j.c.PRF}{4.f_{cl}}$$

or

$$v_{md} = \frac{(j+1).c.PRF}{4.fch} \qquad \text{where } v_{md}\text{, is the new dealiased, ambiguity limit} \tag{12}$$

The ratio $^{j}/_{j} + 1$ can be chosen as low as the frequency resolution in determining $v_{measured}$ will allow. However, small errors in measuring $v_{measured}$ may result in dramatic errors after dealiasing. In the ADCM a (2, 3) frequency pair are the default frequency pair i.e. 250 kHz, 375 kHz, however, a (3, 4) or (4, 5) pair can be nominated.

## Consequences of independent pulses

As stated in (6) a system using m-sequence pulses exhibits a modified spatial resolution. For the ADCM using an 8uS chip length (2 cycles of 250 kHz) the spatial resolution is 12 mm. While allowing more accurate velocity profiling the reduced bin size has the disadvantage that particles will be ensonified for shorter periods of time. Defining the coherence period as the time for which a single particle is resident the PRF must therefore exceed the coherence period for pulse to pulse coherence. A 12 mm bin at the specified maximum velocity $^{5}/_{\sqrt{2}}$ $ms^{-1}$ would require a PRF of at least 290 Hz to meet the pulse to pulse coherence criteria. In practice, to ensure maximum pulse to pulse coherence, the PRF must be as high as possible.

## The echo ranging function

As discussed earlier, it is necessary to provide an echo ranging function within the instrument to detect the surface/water/bed interface. This facility is provided by reconfiguring the instrument to generate sinusoidal tone bursts as transmitted pulses. The receiver then heterodynes the received echoes down to baseband and, after edge enhancement, detects the rising edge of the received pulse. The transmitted pulse is ten cycles of 375 kHz giving a spatial resolution of 40 mm. Since we detect the rising edge of the received pulse and not the envelope, somewhat better resolution can be expected.

## Composite signal structure

Independent m-sequence pulses, phase shift keyed onto the lower of the two carrier frequency pairs, are used to gain a velocity estimate of an ensonified volume at a specified range. The same volume is then ensonified with the upper of the two carrier frequency pairs. The two estimates (possibly aliased) are then used to form an unaliased estimate. The new range velocity ambiguity equation is defined as

$$v_m . r_m = \frac{m.(j+1).c^2}{8 \, f_{ch}} \tag{13}$$

or
$$= \frac{m.j.c^2}{8.f_{cl}}$$

A (250 kHz, 375 kHz) frequency pair i.e. (2, 3) and a pulse multiplicity factor of 6 [11] therefore gives a $v_m r_m$ of 13.5 which, while not exceeding the required 17.6 ($^{25}/\sqrt{2}$), will demonstrate the validity of the system.

## System structure

A block diagram of the system is shown in Fig. 4. Since substantial development was to take place on the system, emphasis was placed on flexibility and replacement of hardware with software where possible. This approach has proven to be invaluable throughout the project.

(i) Signal storage and generation
Real time generation of the transmitted and reference signals is not feasible with current microprocessors, however, the complexity of the signals precludes a hard wired solution. A compromise was arrived at with a temporary storage area of 64 kB static RAM shared between a microprocessor and a sequential counter. In operation, the signals are generated by the microprocessor, written into the RAM, and then sequentially read out by the counter in real time. With a 64 kB RAM and a counter clock of 3 MHz, signals can be generated with delays sufficient to ensonify a volume at a range of 16 meters. The flexibility inherent in this system has allowed us to provide an echo ranging facility as well as a backscatter Doppler sonar in the same instrument.

(ii) Signal processing
Signal processing comprises two sections (a) analogue correlators and (b) the digital spectral transform.

(a) Analogue correlators are provided by multipliers and integrators with integrate and dump facilities. It is important to realise that this configuration does not allow continuous time correlation but only correlation at a defined temporal point. The substantial added complexity of a continuous time correlator was not necessary for this instrument. Analogue correlators were chosen over digital implementations due to their low cost, low power consumption and improved performance.

(b) The digital spectral transform of the output of the correlators is provided by an ADSP-2100 signal processor and analogue to digital convertors. The processor transforms the time domain Doppler signal to the frequency domain and derives the first moment of the resulting spectra. The ADSP-2100 operates at 12.5 MIP's and is capable of real time operation on the received Doppler signals.

(iii) System controller
Overall system control is provided by an Intel 80C196 embedded controller. The system controller generates the transmitted and reference signals in non real time and translates the spectral estimates from the ADSP-2100 into dealiased velocity estimates. It also provides a serial interface to the surface data acquisition system and a real time clock facility.

(iv) Surface data acquisition
The surface data acquisition system is a laptop PC running an instrument configuration and data capture and display programme. Options for instrument configuration are provided with a window based selection procedure and transmitted to the instrument by the serial link. Subsequent data from the instrument is then received and displayed in a graphical format by the PC, a logging facility whereby data is written to disc for later analysis is provided.

## Field results

Field testing of the instrument is still in progress at the time of writing, however, preliminary results appear very promising. Figures 5 to 8 show some data obtained from a recent test at the Water Authority of Western Australia, waste water treatment plant in Shenton Park, Perth. The plant provides a number of conveniently located channels of moving water with a relatively constant velocity and variable suspended particle densities. During the tests, the instrument was mounted at the bottom of a 750 mm channel giving the acoustic path a 45° elevation towards the surface.

(i) Figure 5 shows an echo ranging profile obtained by averaging 256 consecutive pings. The two peaks shown are the backscattered reflections from the water surface and the bed of the channel. From the figure it can be seen that the echoes from the surface and the bed can be easily discriminated from other echoes.
(ii) Figure 6 shows the displacement of the backscattered spectra when the carrier frequency is varied. The dependence of the Doppler frequency on the carrier underlies the dealiasing concept.
(iii) Figure 7 shows a time series of velocity estimates for a single bin. The low variance of the estimates is obvious and compares well with the velocimeter readings (propeller type).
(iv) Figure 8 shows a velocity profile as a function of range. The lower velocities encountered near the surface can be seen. The outlier at a range of 600 mm's is due to sidelobe reflections from the surface and has been described by other researchers [5]. Surface reflections occur with zero Doppler shift and it should therefore be possible to discriminate reflections from stationary objects. Field tests to confirm this are currently in preparation.

### Wider applications

In the wider context, the instrument will be used in coastal circulation investigations (range 20 m, velocity range 1.25 $ms^{-1}$), estuarine research projects (range 5 m, velocity range 5 $ms^{-1}$) and in the study of lake hydrodynamics (range 50 m, velocity range 0.5 $ms^{-1}$). By extending the range ambiguity it has been possible to construct an extremely versatile, highly accurate instrument. Under optimum conditions it will be possible to measure the velocity field with a spatial resolution down to the Kolmogorov scale (for a dissipation of turbulent kinetic energy dissipation of $10^{-7}$ $m^2$ $s^{-3}$) which will enable the resolution of the turbulent field. Thus, the instrument will not only find application in circulation studies, but also in the study of turbulent dispersion.

### Further development

Further development of the principles'developed for the ADCM are planned. A four axis instrument for the three dimensional resolution of bin velocities will be developed. A continuous time correlator will be developed for this instrument to decrease profile acquisition time.

Work is also planned for the optimisation of the code sequences and specifically for the suppression of the spreading code sidelobes by the use of artificial guard sequences.

At the conclusion of the field tests a commercialisation of the ADCM will be undertaken. The cost of the instrument will be minimised and the packaging optimised for end user requirements. Additionally, the software package will be modified so as to remove its developmental aspects and build a useful customer interface.

## CONCLUSIONS

Conventional coherent Doppler backscatter sonars, although ideally suited to the measurement of water velocities, are limited by the range velocity ambiguity equations. This limitation restricts their use at higher water velocities or at longer ranges. The ADCM enhances the basic backscatter system by using noise based pulses and a velocity dealiasing method using two carrier frequencies. These modifications allow the ADCM to be applied to a practical situation where conventional techniques would fail. Preliminary data from field tests has been presented demonstrating the performance of the instrument in deployment conditions.

## ACKNOWLEDGEMENTS

The assistance of the funding partners, the Australian Water Research Council, the Water Authority of Western Australia, and the Main Roads Department, is gratefully acknowledged. The authors also wish to thank Mr Ian Tite of the WAWA, and Dr Saman Abeysekera and Dr Francois Bugnon of the Centre for Water Research for their continued help and enthusiasm.

## REFERENCES

[1] BUGNON, F.J. AND WHITEHOUSE, I.A., Acoustic Doppler Current Meter, University of Western Australia, Centre for Water Research Report ED 352 FB, 1989.

[2] CHAPELON, J.Y., Progress in Medical Imaging, (V.L. Newhouse, editor), Springer Verlag, 1988, Chapter 6.

[3] DIXON, R.C., Spread Spectrum Systems, 2nd edition, Wiley Interscience, 1984.

[4] LEE, B. AND FERGUSON, E., High Speed Digital golay Code Flaw Detection System, Ultrasonics, 1983, 153-161.

[5] LHERMITTE, R.M., Doppler Sonar Observation of Tidal Flow, Journal of Geophysical Research, 1983, 88(C1) 725-742.

[6} LHERMITTE, R.M., Water Velocity and Turbulence Measurements by Coherent Doppler Sonar, Oceans 85 - San Diego, California. Ocean Engineering and the Environment : Conference Record, 1985.

[7] PINKEL, R., Doppler Sonar measurements of Ocean Waves and Currents, Marine Technology Society Journal, 1986, 20(4) pp 58-67.

[8] SHIOZAKI, A., SENDA, S., KITABATAKE, A., INOUE, M. AND MATSUO, H., A New Modulation Method with Range Resolution for Ultrasonic Doppler Flow Sensing. Ultrasonics, 1979, 269-275.

[9] SKAUG, R. AND HJELMSTAD, J.F., Spread Spectrum in Communication, IEE Telecommunication Series, 1985, 12(3) pp. 55-102.

[10] TAKEUSHI, Y., An Investigation of a Spread Energy Method for Medical Ultrasound Systems, Ultrasonics, 1979, 175-224.

[11] WHITEHOUSE, I., Development of an acoustic Doppler current meter, University of Western Australia, Centre for Water Research Report WP 406 IW.

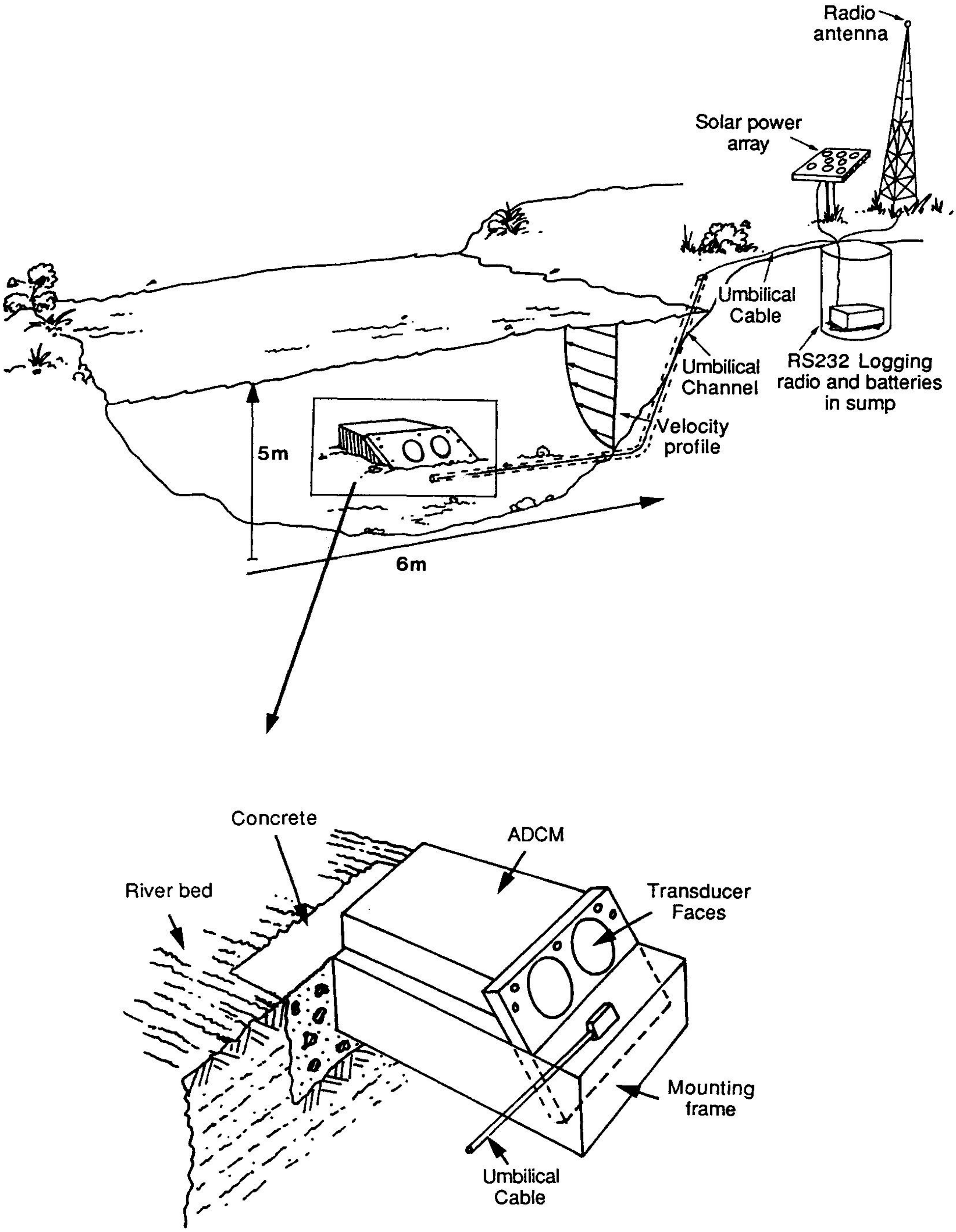


Figure 1. Typical Deployment of ADCM

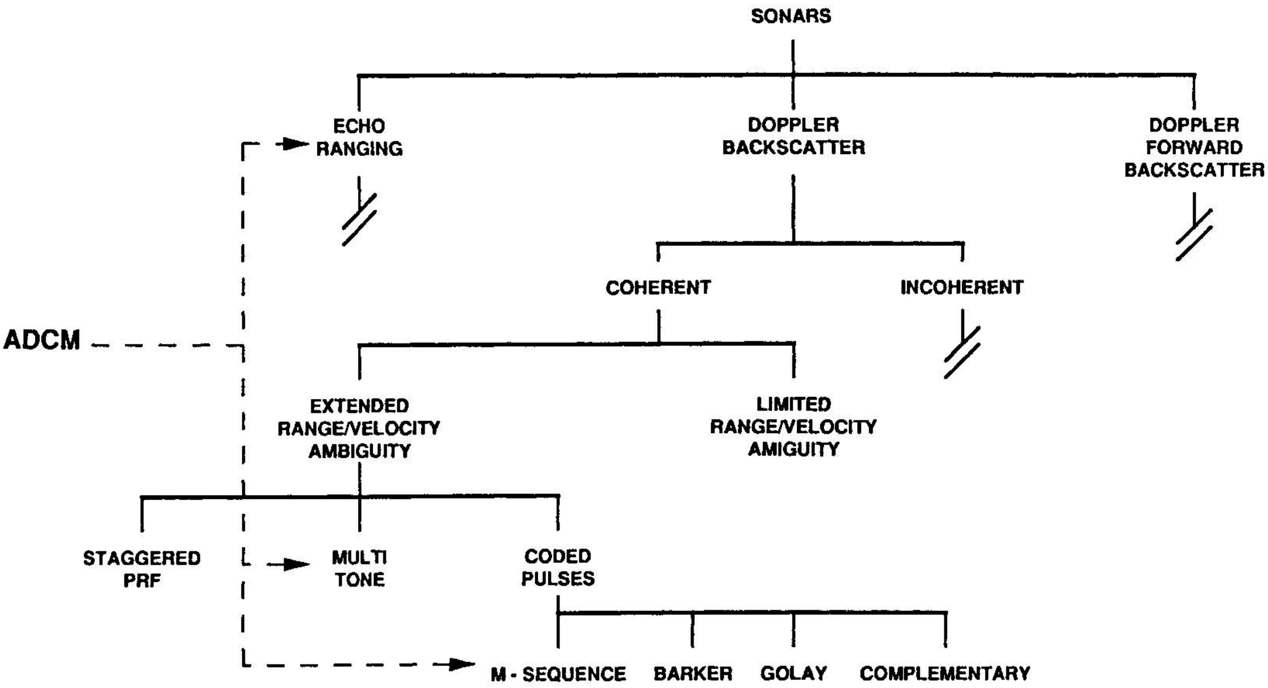


Figure 2. Relationship of ADCM to other sonar systems

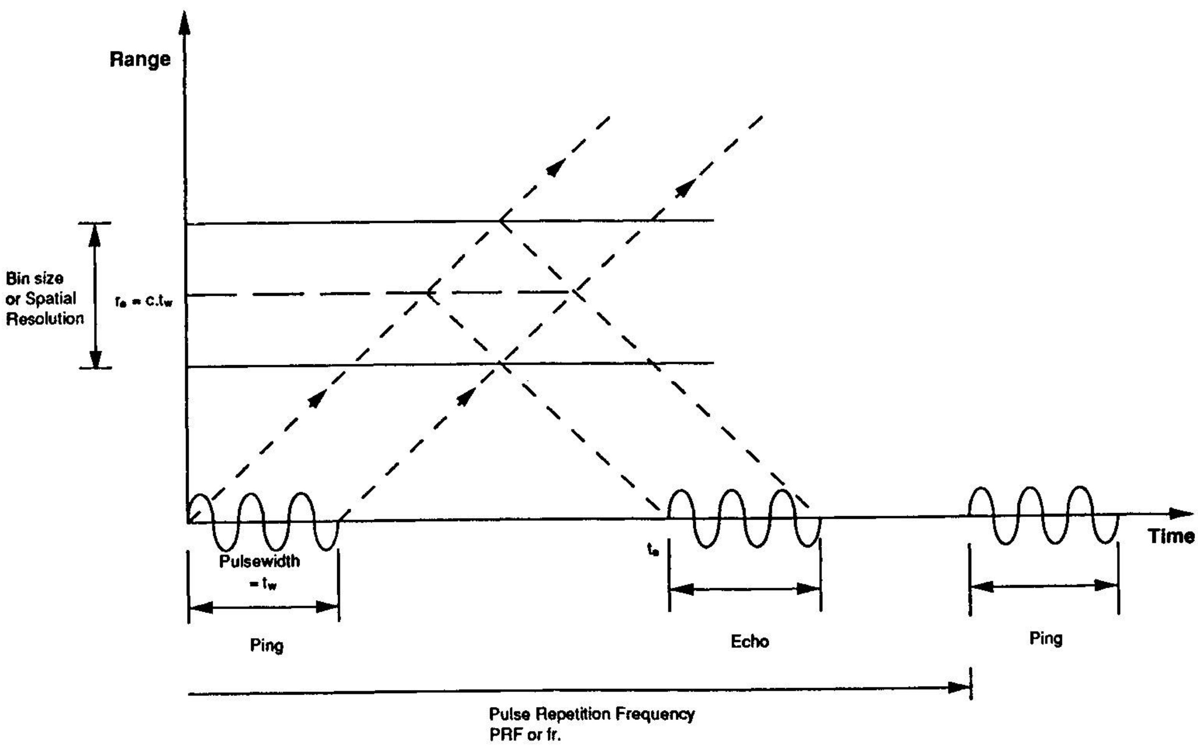


Figure 3. Time/Space diagram for a transmitted pulse

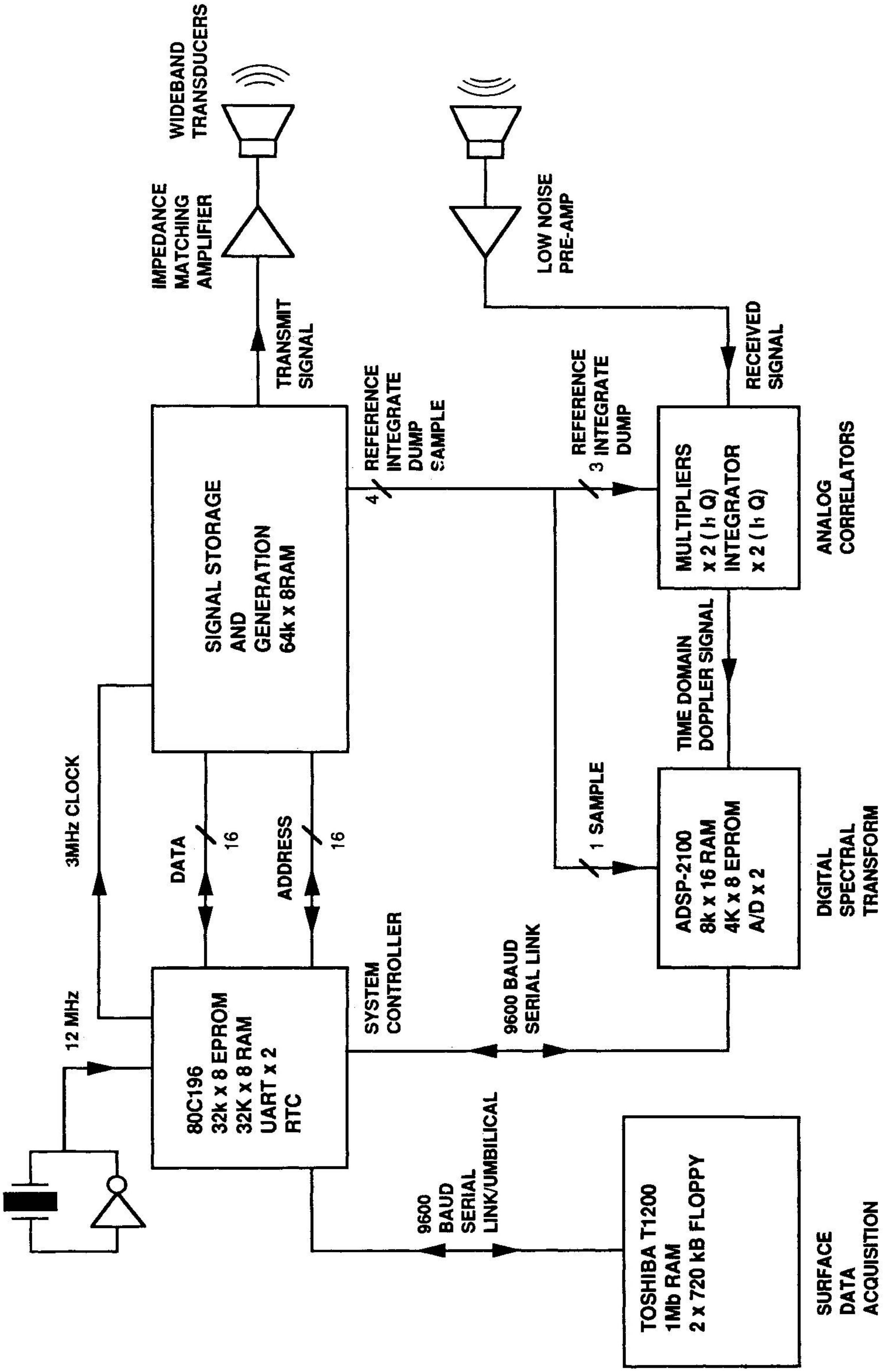


Figure 4. ADCM system diagram

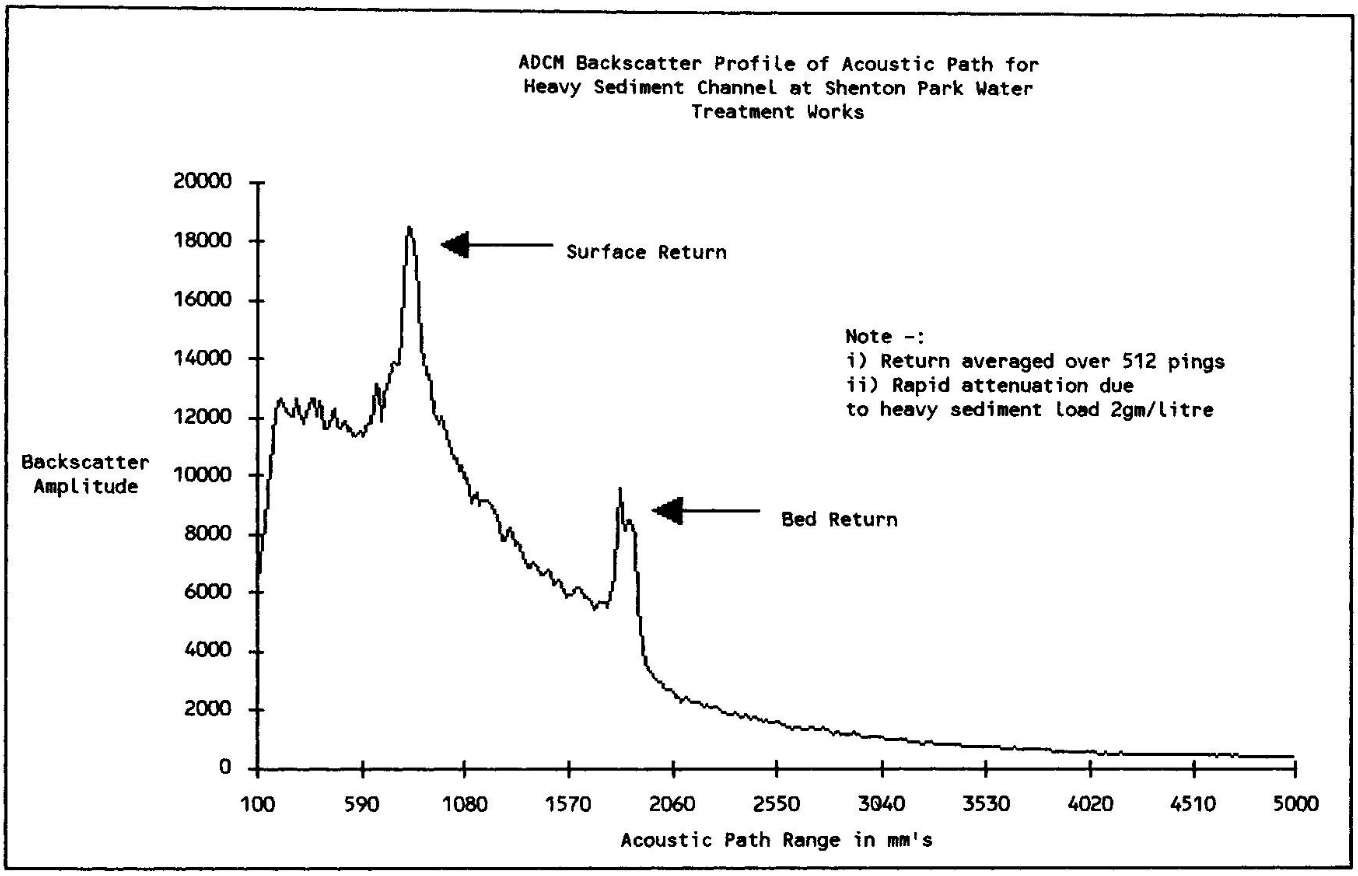


Figure 5.

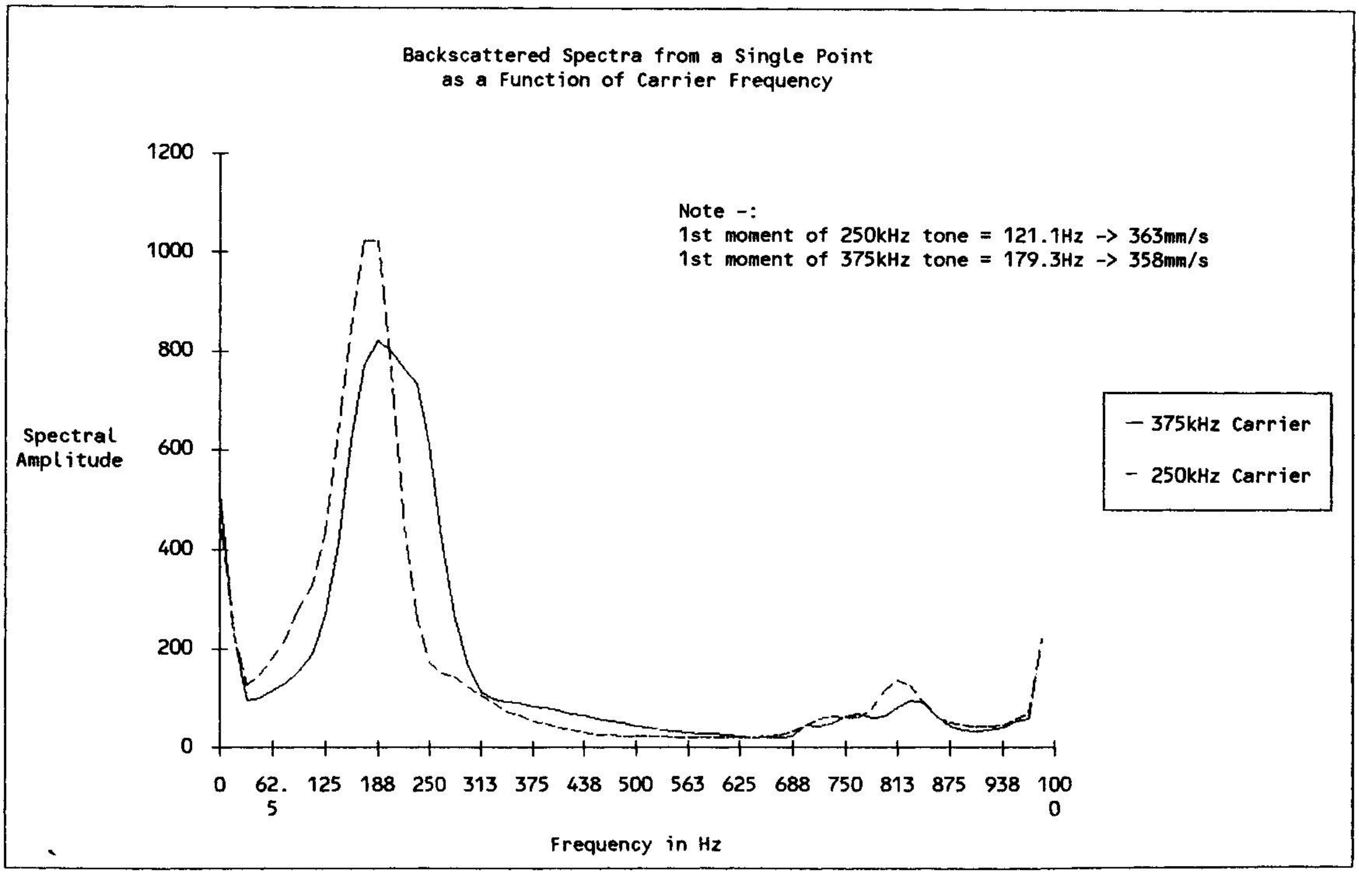


Figure 6.

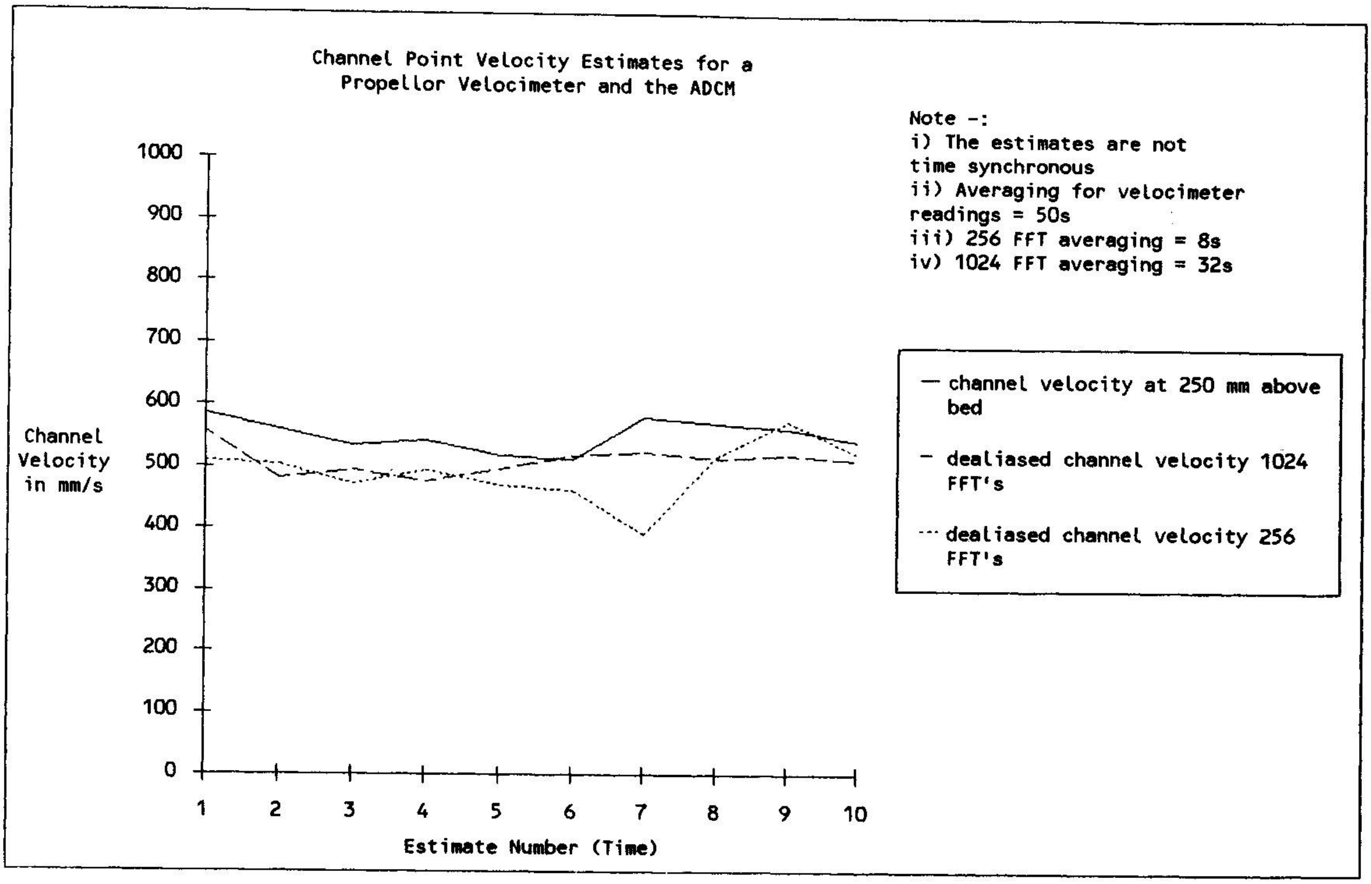


Figure 7.

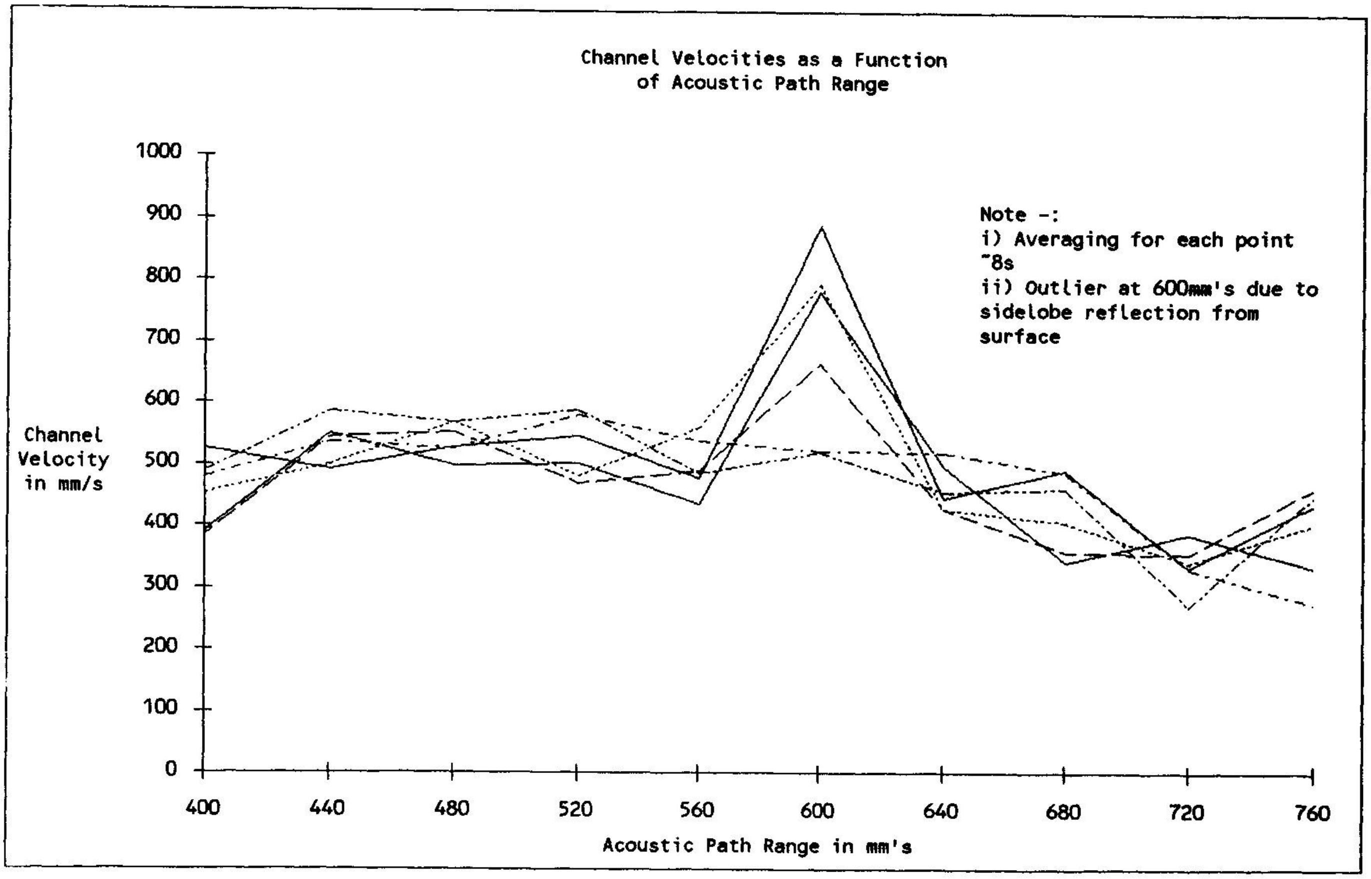


Figure 8.

Leere Seite
Blank page
Page vide